Self-Assembled Fibrillar Networks of Oligo(*p*-phenylenevinylene) Based Organogelators

*Vakayil K. Praveen, Subi J. George, Ayyappanpillai Ajayaghosh**

Summary: Self-assembly induced gelation of a few oligo(*p*-phenylenevinylene) (OPV) derivatives in aliphatic hydrocarbon solvents is described. The gelation is the result of hydrogen bond assisted π-interaction between OPV moieties which facilitate the formation of supramolecular polymeric assemblies, eventually leading to three dimensional fibrillar networks. The number of the aliphatic side chains and the nature of the end functional groups of the OPV backbone play crucial roles in the gelation of hydrocarbon solvents.

Keywords: gelation; hydrogen bonding: oligo(*p*-phenylenevinylene)s; self-assembly; supramolecular structures

Introduction

Small molecule based organogelators in general are three dimensional fibrillar networks composed of one and two dimensional self-assemblies through noncovalent forces associated with hydrogen bonding, π-stacking, van der Waals and dipolar interactions.[1] In most of the cases, the one dimensional supramolecular polymeric assemblies that formed initially will subsequently organize to form nano-to-micrometer sized structures with different morphological features. They immobilize large volume of solvents within the self-assembly to form soft solids, the physical properties of which are in general different from the individual components.

A class of molecules which attracted the attention of supramolecular chemists in recent years is linear π-conjugated systems, mainly due to the favorable optoelectronic properties and applications in organic electronic devices.[2] In this context, self-assembly of oligo(*p*-phenylenevinylene)s (OPV)s have attracted considerable attention of chemists.[3] A few years ago we published the first example of an OPV organogelator which we named as "functional π-gels" of linear conjugated systems.[4] Later we published several papers on OPV based π-gels[5] and demonstrated efficient fluorescent resonance energy transfer (FRET) from OPV gels to entrapped Rhodamine B dye.[6] Herein we show that the gelation of OPVs is strongly dependent upon the nature of the end functional groups, the number of the hydrocarbon chains on the conjugated backbone and the nature of the hydrocarbon solvents used for gelation. The molecules under investigation are shown in Figure 1. They were synthesized as reported earlier and characterized by spectral ananlyses.[5c]

Gelation Properties

Gelation behavior of the OPV derivatives was examined in a range of hydrocarbon solvents by dissolving different amounts in a specific volume (1 mL) of the solvent under heating and cooling. It has been observed that either gelation, precipitation or a clear solution could be obtained depending upon the solvent and structure of the compound. Gel formation could be detected by the failure of the resultant mass to flow when the vial was tilted upside down. The results of the gelation experiments are presented in Table 1, which reveal that the bishydroxy

---

Photosciences and Photonics Unit, Chemical Sciences and Technology Division, Regional Research Laboratory, CSIR, Trivandrum - 695019 (India)
Fax: (+91) 471-2491712
E-mail: aajayaghosh@rediffmail.com

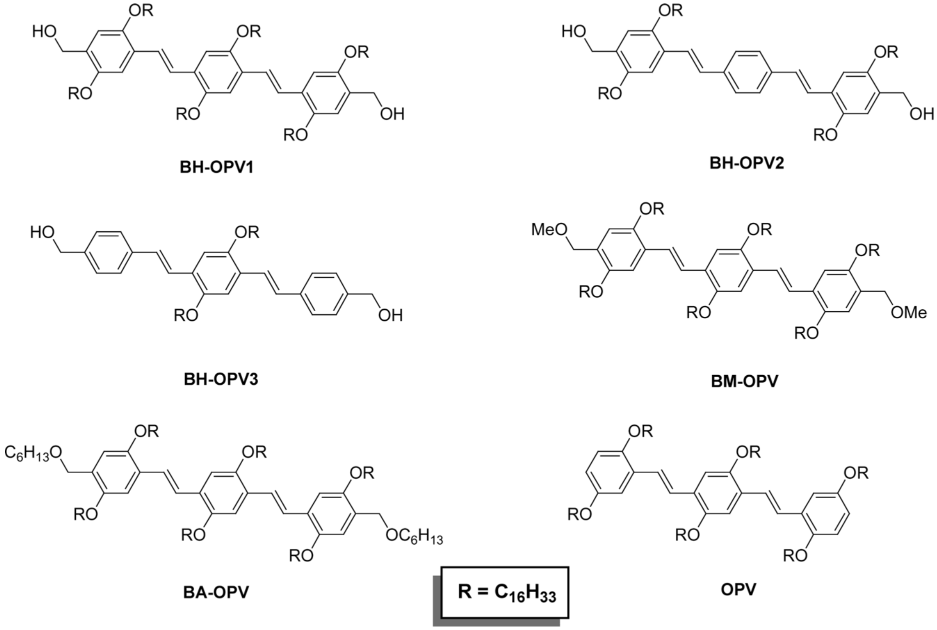

Figure 1.
Molecular structures of OPV derivatives under investigation.

compound **BH-OPV1**, in long chain hydrocarbon solvents is an efficient gelator. For example the critical gelator concentrations (CGC) of **BH-OPV1** in dodecane, decane and cyclohexane were 0.8, 0.9 and 1.1 mM, respectively. This means that **BH-OPV1** can entrap approximately 10,000 molecules of dodecane per gelator molecules and falls under the category of supergelators.[7] Nature of the solvents has considerable influence on the gelation behavior of OPV derivatives. For example, the CGC of **BH-OPV1** in chloroform is 5.6 mM and the resulting gels are unstable upon shaking (thixotropic)[1a] whereas in toluene, a reasonably stable gel with a CGC of 2.8 mM is formed. Another factor, which influences the gelation ability of OPV derivatives, is the number of the hydrocarbon side chains present on the conjugated backbone (Table 1). For instance, the CGC of **BH-OPV2** having side chains only at the terminal phenyl rings is 15.4 mM in cyclohexane resulting in a turbid gel, whereas **BH-OPV3**, with side chains only at the central phenyl ring, does not gelate any of the solvents investigated. Hence, it is clear that for an OPV derivative to form a gel, it is necessary to maintain a balance between crystallization, solubility and precipitation where the length

Table 1.
Critical gelator concentration (CGC)[a] [mM] of OPVs in different solvents.

Gelator	Dodecane	Decane	Cyclohexane	Hexane	Toluene	Benzene	Chloroform
BH-OPV1	0.8 (s, tr)	0.9 (s, tr)	1.1 (s, tr)	1.7 (s, tr)	2.8 (s, tr)	3.0 (s, tr)	5.6 (th, o)
BH-OPV2	PS	PS	15.4 (s, o)	11.5 (s, o)	23.0 (s, o)	PS	PS
BH-OPV3	PS	PS	PS	I	PS	PS	S
BM-OPV	1.6 (th, tr)	1.8 (th, tr)	3.3 (th, tr)	4.4 (th, tr)	7.2 (th, tr)	6.8 (th, tr)	16.5 PG
BA-OPV	4.9 (th, tr)	5.2 (th, tr)	10.4 (th, o)	10.4 (th, o)	S	S	S
OPV	PS	PS	PS	PS	PS	PS	PS

[a] CGC is the minimum concentration required for the formation of a stable gel at room temperature. In parenthesis: s = stable, tr = transparent, th = thixotropic, o = opaque, S = soluble (>25 mgmL^{-1}), I = insoluble, PS = poor solubility, PG = partial gelation at room temperature.

and number of the hydrocarbon side chains play a significant role.

To investigate the role of H-bond assisted π-stacking in the gelation process, we extended our studies to other OPV derivatives where the H-bonding groups are either protected or replaced by other functional groups. The results of the gelation studies of **BM-OPV**, **BA-OPV**, and a simple **OPV** are summarized in Table 1. Interestingly, in the case of the methyl ether derivative **BM-OPV**, gelation occurred only at high concentrations when compared to that of the corresponding hydroxyl derivatives. The CGC of **BM-OPV** in cyclohexane is 3.3 mM, whereas in dodecane and in decane the values are 1.6 and 1.8 mM, respectively. These results indicate that **BM-OPV** is capable of gelating long chain hydrocarbon solvents though the CGC values are almost twice or more when compared to that of **BH-OPV1**. This observation points toward the involvement of weak H-bonding between the methoxy oxygen atoms and the aromatic protons of the benzene rings in long chain hydrocarbon solvents. **BA-OPV**, having hexyloxy end groups, could gelate specifically long chain solvents such as dodecane and decane and the critical gelator concentrations are very high in these cases (<5 mM). The resulting gels are highly unstable and opaque as expected since the hexyloxy end substituents may affect the lamellar type self-assembly in the gel state. However, the **OPV** without any end functional groups could not gelate any of the solvents investigated. Instead aggregate formation was observed which are not able to trap any solvent molecules. These studies point toward the crucial role of H-bonding in assisting π-stacking and van der Waals forces in the process of self-assembly and gelation. At the same time these results open up the possibilities to utilize other weak non H-bonded interactions such as dipolar interactions to the design of new OPV based gelators. Investigations in this direction are in progress and will be published elsewhere.

Thermotropic Behavior

The thermotropic behavior of the gels formed by **BH-OPV1** and **BM-OPV** were investigated by dropping ball method[8] and by differential scanning calorimetry (DSC) to understand the impact of the structure of the OPVs and the nature of the solvents on the gel stability. In the case of **BH-OPV1** and **BM-OPV**, a regular increase in the gel melting temperature (T_{gel}) with increasing concentration of the gelator molecules was observed (Figure 2). Phase diagrams of the OPV gels were obtained by plotting the T_{gel} at different concentrations; the phase above each curve is a solution, whereas the phase below is a gel. Phase diagrams of **BH-OPV1** gels from different solvents are shown in Figure 2a, which indicate that **BH-OPV1** form strong gels in dodecane and cyclohexane, which showed higher melting temperatures even at very low concentrations. This observation is in accordance with the gelation studies presented in Table 1.

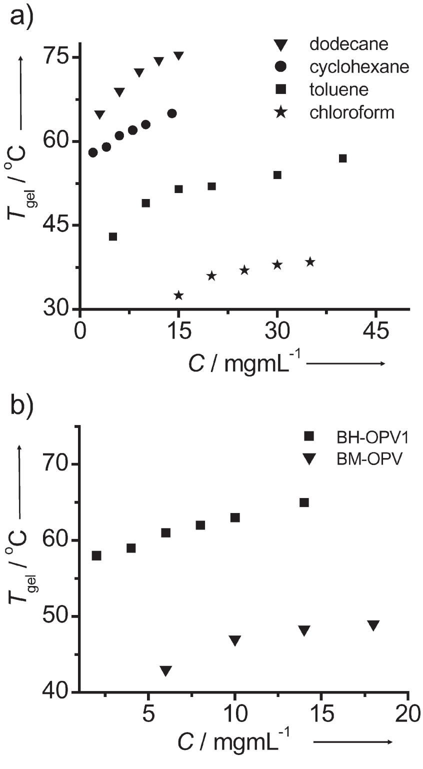

Figure 2.
Phase diagrams of the OPV organogels showing the effect of solvents and H-bonding on stability. a) **BH-OPV1** gels in different solvents and b) cyclohexane gels of **BH-OPV1** and **BM-OPV**.

Figure 2b shows the plots of the gel melting temperatures of the cyclohexane gels of **BH-OPV1** and **BM-OPV** at different concentrations. These plots show remarkable stability for **BH-OPV1** gel, due to H-bonding between the hydroxymethyl groups. For example, a cyclohexane gel of the methoxy derivative **BM-OPV** at a concentration of 10 mgmL^{-1} melts at 47 °C, which is 15 °C lower than the corresponding **BH-OPV1** gel. These results indicate that the stability of the gels strongly depends upon the nature of the solvents and the presence of H-bonding groups.

DSC studies (Figure 3) showed a similar trend in the thermal stability of the gels as observed by the dropping ball methods. A broad exothermic transition was observed during the heating process, which is characteristic of a noncovalently associated supramolecular assembly. In agreement of the dropping ball experiment, the DSC analysis showed increased thermal stability for the gels in hydrocarbon solvents of higher chain length. For example, among the three solvents used, the dodecane gel showed maximum thermal stability (Figure 3a). The role of H-bonding is also evident from the DSC thermograms where **BH-OPV1** showed a melting temperature of 63.5 °C which is 14 °C higher than that of the **BM-OPV** (Figure 3b). In all these cases, it is interesting to note that the cooling transitions are sharper and occurred approximately 15–16 °C lower than the heating transition curves, indicating a better cooperativity in the formation of the self-assembly in the cooling process, leading to the gelation.

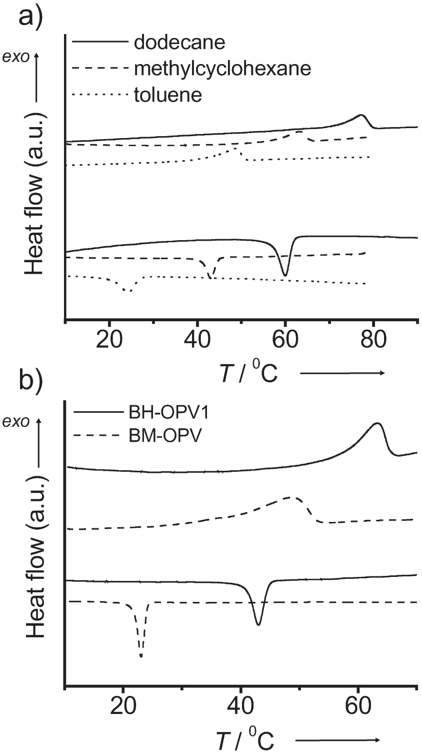

Figure 3.
DSC profiles of a) **BH-OPV1** in different solvents and b) **BH-OPV1** and **BM-OPV** in methylcyclohexane (8 mgmL^{-1}). The heating and cooling rates are 5 °C/min in all experiments.

Optical Polarizing Microscopy

Figures 4a and 4b represent the optical micrographs of a **BH-OPV1** gel in decane under different cooling rates. When cooled from the isotropic solution with a moderate cooling rate of 5 °C min^{-1}, birefringent fibrous aggregates emanating from random nucleation centers could be seen. The strong birefringence of the fibers indicates the anisotropic molecular arrangement during the gelation. When the same experiment was performed at a very low cooling rate of 0.5 °C min^{-1}, slow growth of elongated, birefringent fibers were observed which is evident from Figure 4b, indicating that the cooling rate is critical in the directional growth of the fibrous assembly. Fast cooling induces large number of nucleation sites leading to the radial growth of aggregates whereas slow cooling produces fewer nucleation centers leading to the directional linear growth of long fibers. Interestingly, the decane gels of **BM-OPV** upon slow cooling (0.5 °C min^{-1}) failed to form long fibrous aggregates in contrast to **BH-OPV1**. The difference in the morphology of the structures obtained from the gels of **BH-OPV1** and **BM-OPV** reveals that hydroxymethyl groups are essential for the formation of the extended supramolecular assemblies with long range

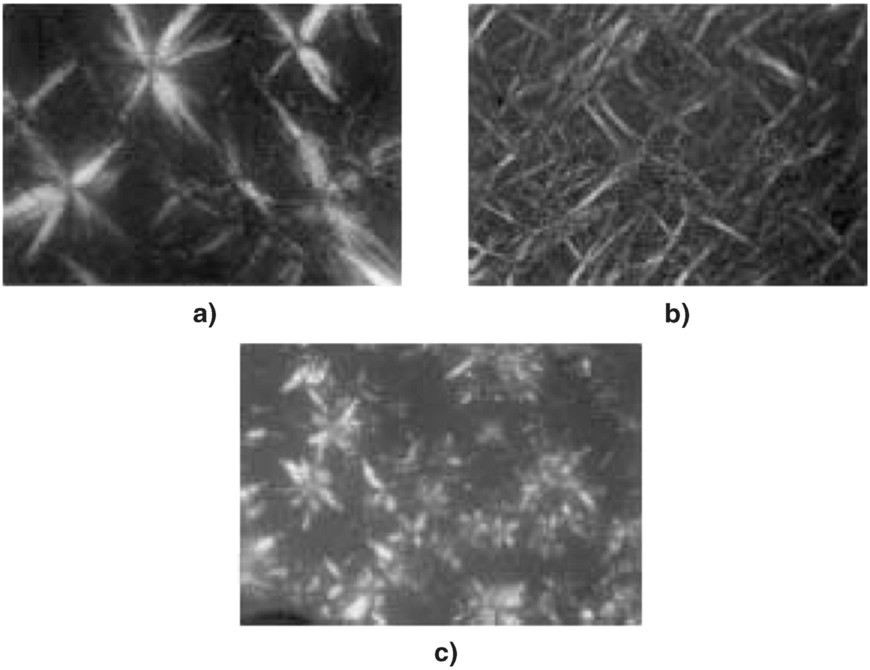

Figure 4.
Optical micrographs of the decane gels of **BH-OPV1** under a) moderate cooling, b) slow cooling and c) **BM-OPV** decane gel observed under slow cooling.

ordering, leading to fiber growth and efficient gelation.

Scanning Electron Microscopic Studies

Detailed scanning electron microscopic (SEM) investigation of the different OPV organogels provided insight to the role of H-bonding functionality on their self-assembled architectures. SEM images of a dried **BH-OPV1** gel from cyclohexane showed supramolecular fibrous nanostructures (Figure 5a). The fibers are of approximately 50–200 nm in width and several micrometers in length. The long fibers are the result of the co-operative hydrogen boning and π-π stacking interactions. In the case of the methyl ether derivative **BM-OPV**, short fibrous aggregates are obtained (Figure 5b). This observation is in contrast to the several micrometers long fibers of **BH-OPV1** gels. A SEM picture of a film of **OPV** having no end substituents showed a completely different morphology, in which randomly clustered large aggregates of 0.5–1.0 μm in size are present (Figure 5c). These aggregates failed to trap organic solvents and hence **OPV** was not able to form gels. The above observations indicate that H-bond formation between the terminal hydroxymethyl groups is a key factor for the efficient gelation of OPVs, leading to the formation of supramolecular textures of long-range order.

Absorption and Emission Properties

The electronic absorption and emission properties of OPVs are ideal tool to monitor the self-assembling process. The most important feature of the gelation of OPVs is the self-assembly induced modulation of optical properties. The absorption and emission spectra of OPVs under different experimental conditions are shown in Figure 6. In the case of **BH-OPV1** (Figure 6a) the absorption and emission spectra of a dodecane solution at 20 °C showed considerable resemblence to that of a casted film indicating nearly identical

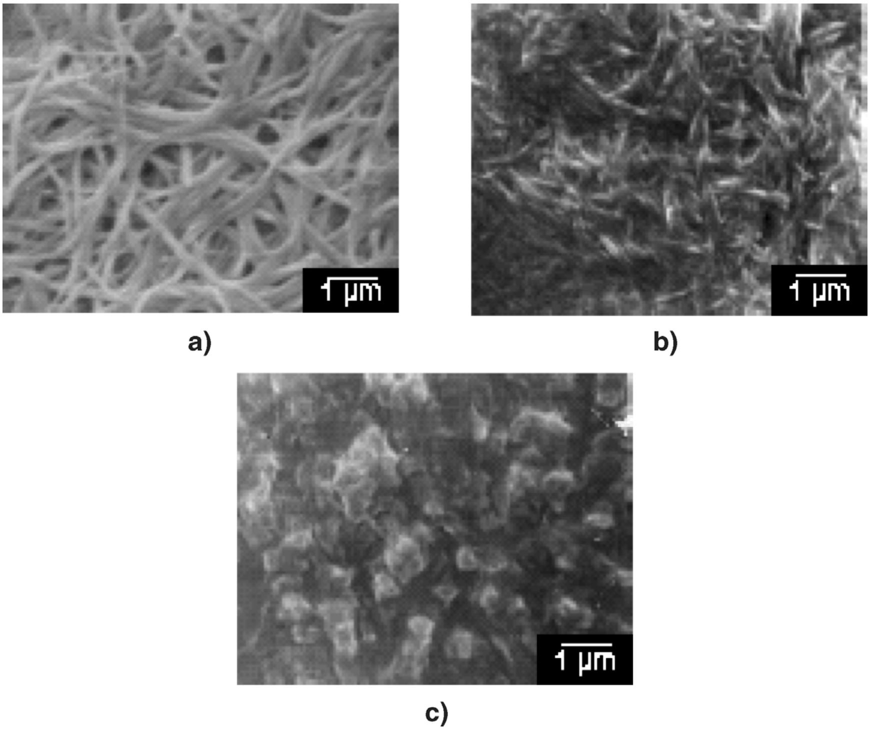

Figure 5.
SEM pictures of cyclohexane gel of a) **BH-OPV1** b) **BM-OPV** and c) **OPV**.

chromophore packing in both cases. To establish this, we have recorded the absorption and emission spectra of **BH-OPV1** in dodecane at 65 °C, which resembled to the spectra in chloroform. These observations imply that **BH-OPV1** is in the self-assembled states in dodecane at 20 °C whereas at elevated temperatures the self-assembly is broken to form molecularly dissolved species. In cylcohexane at room temperature **BH-OPV1** showed a broad emission with several maxima at 454, 476, 527 and 561 nm, the relative intensities of which are dependent upon temperature and concentration (Figure 6a). This observation indicates the possibility of more than one co-existing species. **BM-OPV** in cyclohexane (Figure 6b) showed an emission spectrum with maxima around 452 and 480 nm, which has a close resemblence to the spectrum of moleculerly dissolved species. However, in dodecane and in the in the film form significant shift in the emission could be seen. This means that the self-assembly of **BM-OPV** is efficient only in long chain aliphatic solvents which is in agreement with the gelation and the morpholoical studies. In the case of the simple **OPV** (Figure 6c) in dodecane at 20 °C, a red-shifted shoulder at 465 nm is observed whereas the emission maxima are not shifted significantly. The emission spectrum in decane at 20 °C has no resemblence with that of the solid state, which further indicates the differnces in chromophore packing in the aggregate form in solution.

Conclusions

In conclusion, we have shown the effect of the number of the hydrocarbon side chains of the conjugated backbone, the role of the H-bonding end groups and the nature of the hydrocarbon solvents in the self-assembly

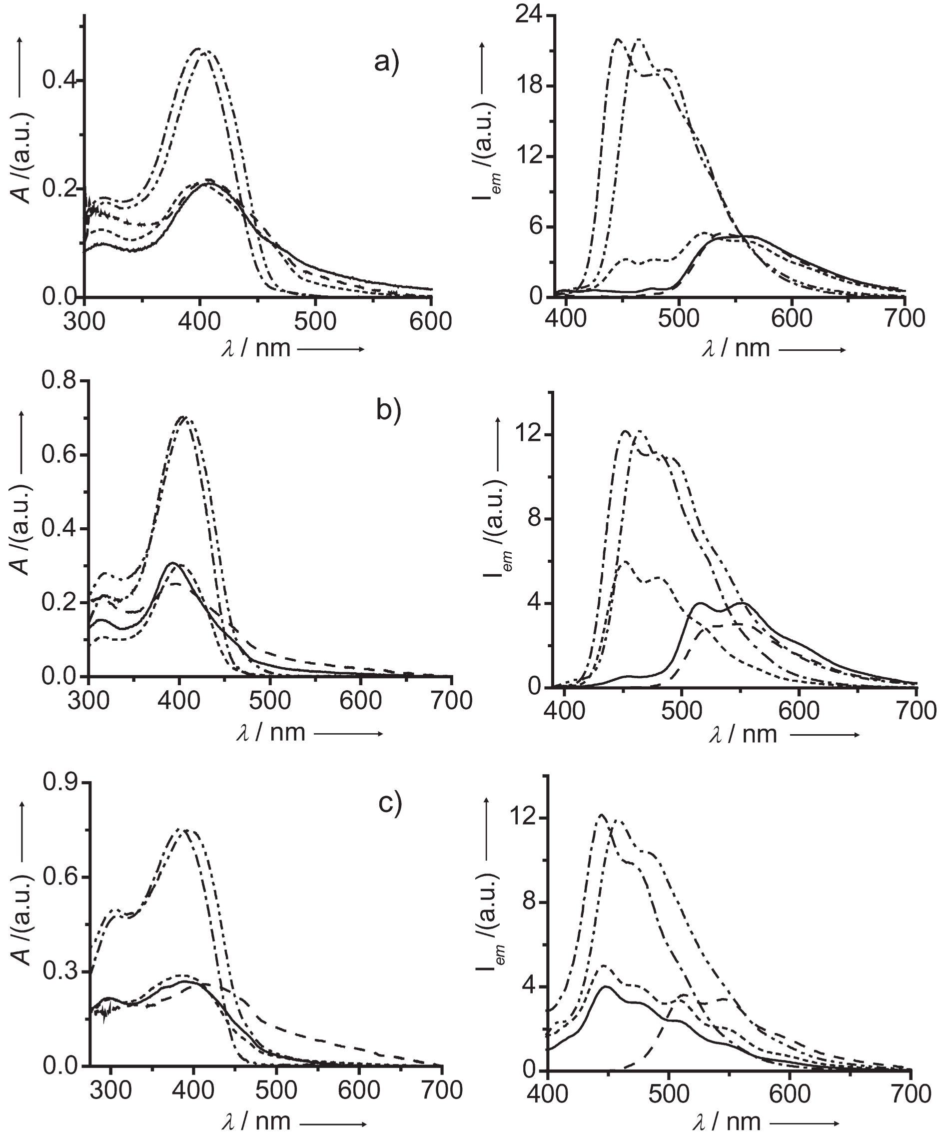

Figure 6.
Absorption (left) and emission (right) spectra of a) **BH-OPV1**, b) **BM-OPV** and c) **OPV** under different conditions. In chloroform (-..-..-), cyclohexane (⋯⋯), dodecane at 20 °C (‾), dodecane at 65 °C (-.-.-.) and in the solid state (-----). In all the experiments concentration of OPV derivatives is (1×10^{-5} M) and $\lambda_{ex} = 380$ nm.

and gelation of a few OPV derivatives. They form fibrillar self-assemblies in aliphatic hydrocarbon solvents resulting in the gelation of the solvent. **BH-OPV1** with two C_{16} side chains on each aromatic ring showed maximum gelation in dodecane whereas the removal of two of the side chains from the middle benzene ring, (**BH-OPV2**) significant decreased the gelation ability. **BH-OPV3** with two C_{16} side chains failed to gelate any of the solvent tested. **BM-OPV** with two methoxy end groups showed weak gelation in comparison to that of **BH-OPV1**. As a result of the self-assembly, significant modulation of the optical properties could be achieved which was dependent up on the structure of the molecules. The difference in the gel melting temperatures, optical properties and the morphologies of the self-assemblies of these compounds reveal the importance of H-bonding in assisting the π-interactions in the formation of extended supramolecular structures.

Acknowledgements: This work was supported by the Department of Science and Technology (DST), Government of India, and the Council of Scientific and Industrial Research (CSIR) Task Force Program (CMM 010). V.K.P. thanks the CSIR for a research fellowship. This is manuscript No. RRL-PPU-214.

[1] For reviews on low molecular weight organogels, see: [1a] P. Terech, R. G. Weiss, *Chem. Rev.* **1997**, *97*, 3133; [1b] J. H. van Esch, B. L. Feringa, *Angew. Chem. Int. Ed.* **2000**, *39*, 2263; [1c] L. A. Estroff, Hamilton, A. D. *Chem. Rev.* **2004**, *104*, 1201; [1d] T. Ishi-i, S. Shinkai, *Top. Curr. Chem.* **2005**, *258*, 119; [1e] N. M. Sangeetha, U. Maitra, *Chem. Soc. Rev.* **2005**, *34*, 821.

[2] For reviews on π-conjugated systems, see: [2a] F. J. M. Hoeben, P. Jonkheijm, E. W. Meijer, A. P. H. J. Schenning, *Chem. Rev.* **2005**, *105*, 1491; [2b] A. P. H. J. Schenning, E. W. Meijer, *Chem. Commun.* **2005**, 3245; [2c] A. Ajayaghosh, S. J. George, A. P. H. J. Schenning, *Top. Curr. Chem.* **2005**, *258*, 83.

[3] [3a] J.-F. Eckert, J.-F. Nicoud, D. Guillon, J.-F. Nierengarten, *Tetrahedron Lett.* **2000**, *41*, 6411; [3b] A. P. H. J. Schenning, J. van Herrikhuyzen, P. Jonkheijm, Z. Chen, F. Würthner, E. W. Meijer, *J. Am. Chem. Soc.* **2002**, *124*, 10252; [3c] P. Jonkheijm, F. J. M. Hoeben, R. Kleppinger, J. van Herrikhuyzen, A. P. H. J. Schenning, E. W. Meijer, *J. Am. Chem. Soc.* **2003**, *125*, 15941; [3d] P. Jonkheijm, A. Miura, M. Zdanowska, F. J. M. Hoeben, S. De Feyter, A. P. H. J. Schenning, F. C. De Schryver, E. W. Meijer, *Angew. Chem. Int. Ed.* **2004**, *43*, 74; [3e] B. W. Messmore, J. F. Hulvat, E. D. Sone, S. I. Stupp, *J. Am. Chem. Soc.* **2004**, *126*, 14452; [3f] J. F. Hulvat, M. Sofos, K. Tajima, S. I. Stupp, *J. Am. Chem. Soc.* **2005**, *127*, 366; [3g] M. Wolffs, F. J. M. Hoeben, E. H. A. Beckers, A. P. H. J. Schenning, E. W. Meijer, *J. Am. Chem. Soc.* **2005**, *127*, 13484.

[4] A. Ajayaghosh, S. J. George, *J. Am. Chem. Soc.* **2001**, *123*, 5148.

[5] [5a] S. J. George, A. Ajayaghosh, P. Jonkheijm, A. P. H. J. Schenning, E. W. Meijer, *Angew. Chem. Int. Ed.* **2004**, *43*, 3421; [5b] R. Varghese, S. J. George, A. Ajayaghosh, *Chem. Commun.* **2005**, 593; [5c] S. J. George, A. Ajayaghosh, *Chem. Eur. J.* **2005**, *11*, 3217.

[6] A. Ajayaghosh, S. J. George, V. K. Praveen, *Angew. Chem. Int. Ed.* **2003**, *42*, 332.

[7] R. Luboradzki, O. Gronwald, A. Ikeda, S. Shinkai, *Chem. Lett.* 2000, 1148.

[8] In a dropping ball method, a steel ball (150 mg) was placed on the top of a 1 mL volume gel in a sealed glass vial. Then the gels were slowly heated, while the position of the ball on the top of gel is continuously observed, until the gel no longer bears the ball. The temperature at which the ball reaches the bottom of vial is taken as the sol-gel phase transition temperature (T_{gel}).